Journal of Organometallic Chemistry, 417 (1991) 9–27
Elsevier Sequoia S.A., Lausanne
JOM 21925

ansa-Metallocene derivatives

XXIII *. Aryl-substituted titanocene and zirconocene complexes with interannular tetramethylethano- or dimethylsilano-bridges. Crystal structures of representative examples **

Peter Burger, Kai Hortmann, Josef Diebold and Hans-Herbert Brintzinger *
Fakultät für Chemie, Universität Konstanz, W-7750 Konstanz (Germany)

(Received March 7th, 1991)

Abstract

Titanocene and zirconocene complexes with a phenyl or 1-naphthyl substituent in one β-position of each C_5-ring ligand and with an interannular tetramethylethano- or dimethylsilano-bridge have been prepared. Racemic complex isomers, which are formed together with varying amounts of their *meso* isomers, were separated from the latter and characterised by ^1H NMR spectroscopy and X-ray crystallographic studies.

Introduction

Pino and his collaborators [1] have greatly contributed to our understanding of homogeneous Ziegler–Natta catalysts of the *ansa*-zirconocene type [2], especially in respect of the origin of stereoselectivity in these reaction systems. Through their studies of the stereochemical course of α-olefin hydro-oligomerisation catalysed by optically-resolved chiral *ansa*-metallocenes [3], Pino and coworkers provided convincing evidence for a plausible concept of the catalytic site in homogeneous polymerisation catalysts [4]. This concept stimulated further efforts to clarify the interrelations between molecular structures of chiral *ansa*-metallocenes and their properties as α-olefin polymerisation catalysts. While *ansa*-zirconocene derivatives with β-alkyl substituents have subsequently been studied in some detail [5,6], β-aryl-substituted complexes of this type seem not to have been investigated previously. In extension of our studies of structure–reactivity correlations in this field, we report here the syntheses and crystal structures of several *ansa*-metallocene

* For Part XXII see ref. 15.
** Dedicated to the memory of Professor Piero Pino.

0022-328X/91/$03.50

derivatives that have a phenyl or 1-naphthyl substituent in the β-position of their tetramethylethano- or dimethylsilano-bridged cyclopentadienyl ligands.

Ligand syntheses

We previously observed that an additional methyl substituent in α-position of each cyclopentadienyl ligand, next to the inter-annular bridge, increased the diastereoselectivity of the ensuing complex formation in favour of the racemic isomer [7]; our syntheses were thus aimed at 2-methyl-4-aryl-substituted, ethano- and silano-bridged bis(1-cyclopentadienyl) dianion ligands, with the tetramethylethano-bridge to be generated by reductive coupling [8,9] of the corresponding dimethylfulvene derivative *.

3-Methyl-1-phenyl- and 3-methyl-1-naphthyl-cyclopentadiene (**1a,b**), prepared in 80 and 65% yield, respectively, with some modifications, by previously described procedures [11,12], were converted into their 6,6-dimethylfulvene derivatives (**2a,b**) by pyrrolidine-induced condensation with acetone [13] in > 90% yield. Reductive coupling with Mg/CCl_4 gave the Grignard derivatives **3a,b** in 15% yield (Scheme 1).

Alternatively, dimethylsilyl-bis(2-methyl-4-phenyl-cyclopentadiene), formed by reaction of the lithium salt of **1a** with dimethyldichlorosilane, was deprotonated *in situ* with n-butyllithium to give the dilithium salt **4**, which was used for the subsequent complex formation reaction without isolation (Scheme 2).

Complex formation

Reaction of the Grignard reagent **3a** with $TiCl_3 \cdot 3THF$ in tetrahydrofuran (THF) gave complexes **5a** and **6** in about 15% yield, with a *rac/meso* isomer ratio of ca. 6/1. Conversion of **3a** into the di-lithium salt and subsequent reaction with $TiCl_3 \cdot 3THF$ in THF doubled the total yields to ca. 30% while lowering the *rac/meso* ratio to ca. 2/1. By treating **3a** with $TiCl_4$ in toluene the total yields were further increased to 40%, but the *rac/meso* ratio fell further to 1/1.

The chiral *ansa*-zirconocene **7a** was similarly prepared by reaction of **3a** with $ZrCl_4 \cdot 2THF$ in THF. In this case, only the racemic complex was isolated, in ca. 10% yield. Exclusive formation of the racemic isomer, isolated in ca. 8% yield, was also observed in the case of the naphthyl-substituted *ansa*-titanocene **5b** **, in the reaction of **3b** with $TiCl_3 \cdot 3THF$ in THF (Scheme 3).

The dimethylsilano-bridged phenyl-substituted zirconocene complexes **8** and **9**, were obtained in 12% total yield by reaction of the dimethylsilano-bridged dilithium salt **4** with $ZrCl_4 \cdot 2THF$ in THF, with a *rac/meso* isomer ratio of ca. 1/1 (Scheme 3).

Pure samples of the racemic *ansa*-metallocene derivatives **5a**, **5b**, **7a** and **8** were obtained by fractional crystallisation. They were characterised by determination of their crystal structures (see next section) and from their mass and ^1H NMR spectra and elemental analyses ***. The assignments of the α- and β-^1H NMR signals

---

* Alternative routes to ethano-bridged, chiral *ansa*-metallocenes have been described by Collins and his coworkers [10].

** The naphthyl-substituted *ansa*-zirconocene **7b** was observed in the ^1H NMR spectrum of the product mixture after reaction of **3b** with $ZrCl_4 \cdot 2THF$ in THF, but could not be isolated.

*** Compounds **5a** and **7a** crystallise with inclusion of one molecule of CH_2Cl_2 per molecule of complex.

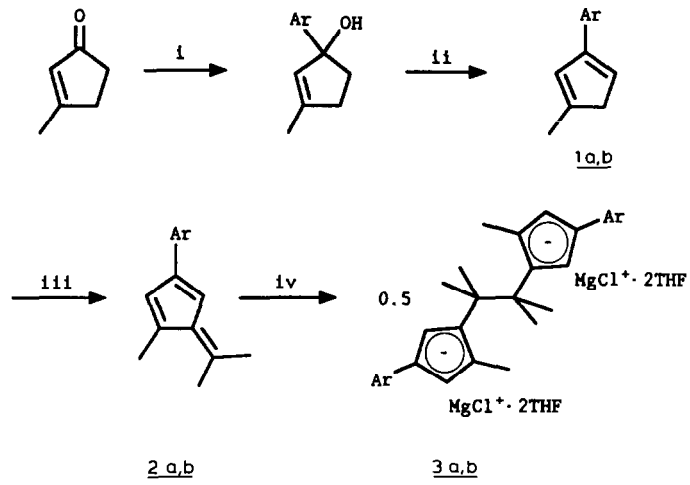

Ar	i	ii	iii	iv
a phenyl	1) LiC_6H_5 (excess), in Et_2O, 0 → 20°C 2) H_2O	100 → 160°C (10 Torr), total yield (i,ii): 80%	acetone, pyrrolidine (RT, 5h) yield: 95%	Mg/CCl_4, THF yield: 15%
b 1-naphthyl	1) 1-$LiC_{10}H_7$ in Et_2O, 0 → 20°C 2) H_2O	180°C (10^{-2} Torr) or p-TsOH in Et_2O, total yield (i,ii): 65%	acetone, pyrrolidine (RT, 14h) yield: 90%	Mg/CCl_4, THF yield: 15%

Scheme 1.

shown in Table 1, confirmed by nuclear Overhauser enhancement of the respective α-signal upon irradiation at the resonance frequency of the bridge-CH_3 groups, are in accord with established rules [14].

Complex **5a** was further identified as the racemic isomer by its conversion upon treatment with 2 equivalents of CH_3Li into its dimethyl derivative, which gives only one $Ti(CH_3)_2$ ^1H NMR signal, at -0.28 ppm, in $CDCl_3$.

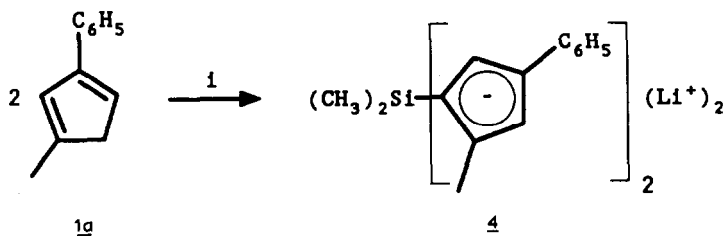

Scheme 2. i: 1) 2 eq. ^{n}BuLi, 2) 1 eq. $Si(CH_3)_2Cl_2$, 3) 2 eq. ^{n}BuLi.

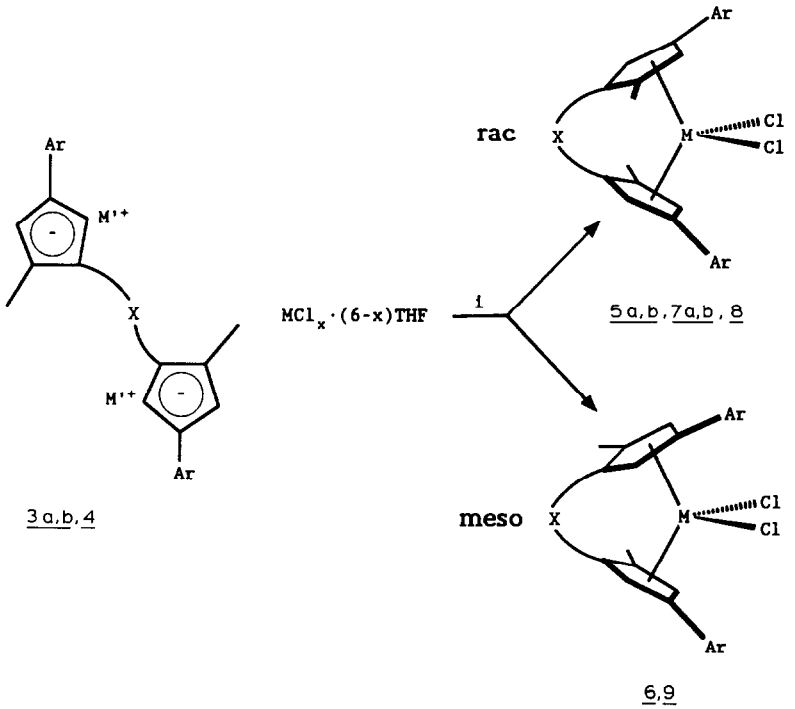

	5a	5b	6	7a	7b	8	9
M'	MgCl or Li	MgCl	MgCl or Li	MgCl	MgCl	Li	Li
X	$C_2(CH_3)_4$	$C_2(CH_3)_4$	$C_2(CH_3)_4$	$C_2(CH_3)_4$	$C_2(CH_3)_4$	$Si(CH_3)_2$	$Si(CH_3)_2$
Ar	phenyl	1-naphthyl	phenyl	phenyl	1-napthyl	phenyl	phenyl
M	Ti	Ti	Ti	Zr	Zr	Zr	Zr
	rac	rac	meso	rac	rac	rac	meso

Scheme 3. i: for reaction conditions and yields see text.

Crystal and molecular structures

Crystal and molecular structures for complexes **5a**, **5b**, **7a** and **8** were determined by X-ray diffraction. The resulting structural data (Fig. 1–4, Tables 2–5) confirm the ^{1}H NMR identification of these complexes as the racemic species. Coordination geometries around the metal centres, i.e. metal–chloride and metal–carbon distances as well as chloride–metal–chloride and ring centroid–metal–centroid angles, are all within the range normally found for complexes of this type.

For all of the complexes studied the molecular framework shows the expected axial symmetry: The interannular bridges are found to lie either exactly on (**5a**, **5b**)

Table 1

^{1}H NMR data for *rac*- (**5a,b,7a,8**) and *meso*- (**6,9**) configurated *ansa*-metallocenes (X[1-C_5H_2-2-CH_3-4-R]$_2MCl_2$, X = Me_2Si and CMe_2Me_2C, M = Ti, Zr) in $CDCl_3$ solution at 298 K, δ in ppm (relative to δ ($CHCl_3$) 7.24 ppm) at 250 MHz (s = singlet, d = doublet with $J(H_\alpha,H_\beta) \approx 2.7$ Hz, m = multiplet)

Me = Ti		M = Zr	M = Ti	M = Zr		Assignment
X = CMe_2Me_2C, R = C_6H_5		X = CMe_2Me_2C, R = C_6H_5	X = CMe_2Me_2C, R = 1-$C_{10}H_7$	X = Me_2Si, R = C_6H_5		
rac (**5a**)	*meso* (**6**)	*rac* (**7a**)	*rac* 95**b**)	*rac* (**8**)	*meso* (**9**)	
				0.90 (s,6)		1-Si(CH_3)
					0.80 (s,3)	1-Si(CH_3)
					1.01 (s,3)	1-Si(CH_3)
1.52 (s,6)	1.55 (s,6)	1.53 (s,6)	1.69 (s,6)			1,1′-$C_2(CH_3)_4$
1.71 (s,6)	1.67 (s,6)	1.70 (s,6)	1.75 (s,6)			1,1′-$C_2(CH_3)_4$
2.35 (s,6)	2.45 (s,6)	2.41 (s,6)	2.39 (s,6)	2.20 (s,6)	2.34 (s,6)	2-CH_3
6.23 (d,2)	6.62 (d,2)	6.27 (d,2)	6.25 (d,2)	5.85 (d,2)	5.83 (d,2)	5-C_5H_2
6.85 (d,2)	6.69 (d,2)	6.65 (d,2)	7.08 (d,2)	6.97 (d,2)	6.80 (d,2)	3-C_5H_2
7.26–7.46 (m,10)	7.16–7.34 (m,10)	7.22–7.45 (m,10)		7.20–7.42 (m,10)	7.20–7.42 (m,10)	4-C_6H_5
			7.44–7.56 (m,6)			4-(1-$C_{10}H_7$)
			7.66–7.69 (m,2)			4-(1-$C_{10}H_7$)
			7.80–7.87 (m,4)			4-(1-$C_{10}H_7$)
			8.54–8.57 (m,2)			4-(1-$C_{10}H_7$)

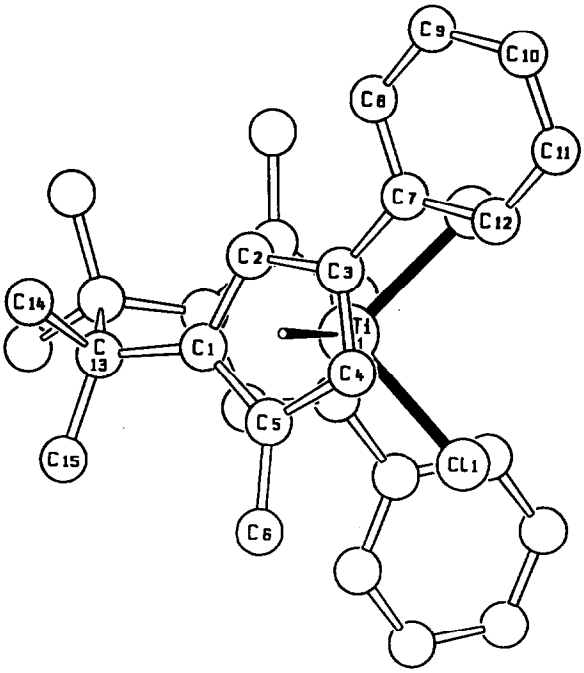

Fig. 1. Structure of $(CH_3)_4C_2[1R\text{-}C_5H_2\text{-}2\text{-}CH_3\text{-}4\text{-}C_6H_5]_2TiCl_2$ (**5a**); projection normal to the $TiCl_2$ plane.

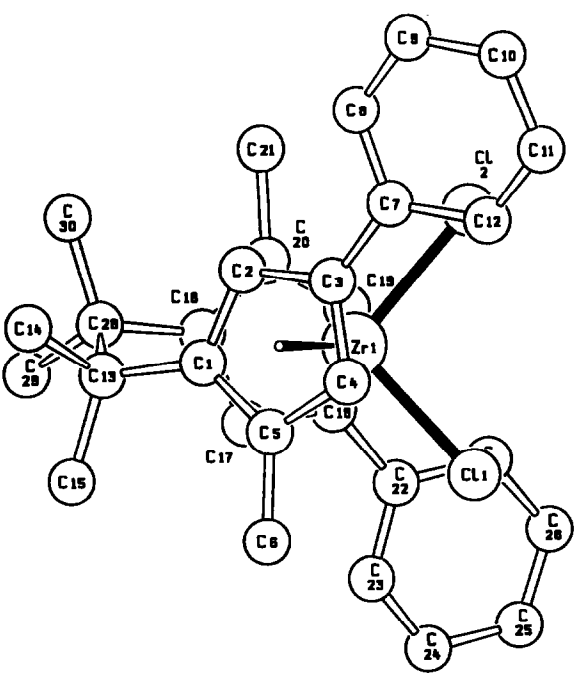

Fig. 2. Structure of $(CH_3)_4C_2[1R\text{-}C_5H_2\text{-}2\text{-}CH_3\text{-}4\text{-}C_6H_5]_2ZrCl_2$ (**7a**); projection normal to the $ZrCl_2$ plane.

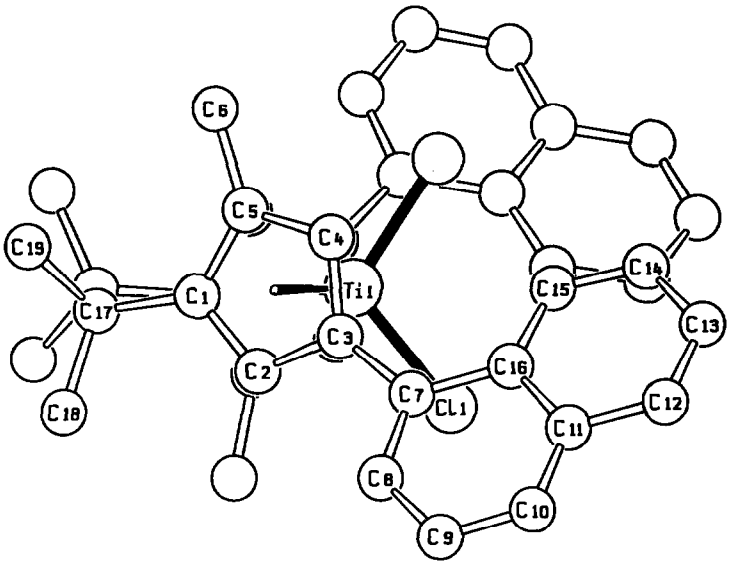

Fig. 3. Structure of $(CH_3)_4C_2[1\text{-}C_5H_2\text{-}2\text{-}CH_3\text{-}4\text{-}(1\text{-}C_{10}H_7)]_2TiCl_2$ (**5b**) (the 1*S*-enantiomer is represented); projection normal to the $TiCl_2$ plane.

or close to (**7a**, **8**) the rear extension of the $TiCl_2$ or $ZrCl_2$ bisector axes. This axially symmetric arrangement contrasts with non-axial distortions observed in other *ansa*-metallocenes bearing more bulky β-substituents [9,10]. Non-bonding intramolecular distances between aryl-C atoms and Cl ligands fall below the van der Waals limit in some cases but less so than is the case for bulkier alkyl substituents [7,9,10].

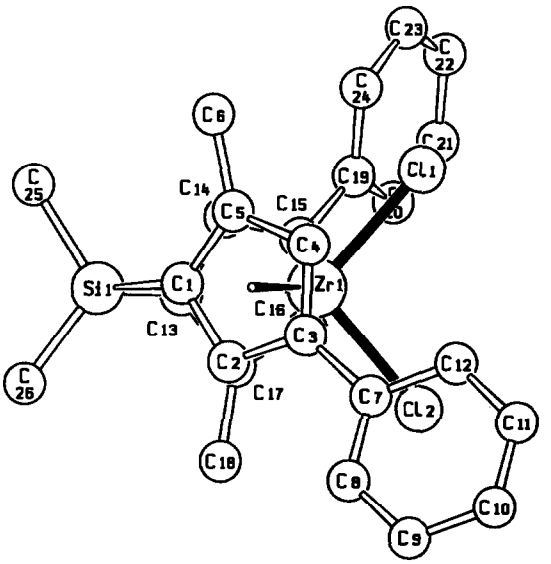

Fig. 4. Structure of $(CH_3)_2Si[1\text{-}C_5H_2\text{-}2\text{-}CH_3\text{-}4\text{-}C_6H_5]_2ZrCl_2$ (**8**); (the 1*S*-enantiomer is represented); projection normal to the $ZrCl_2$ plane.

Table 2

Bonding and non-bonding distances (pm), bond and dihedral angles (°) with esd's in parentheses for complex **5a**, *rac*-$C_2(CH_3)_4$[1-R-(δ)-C_5H_2-2-CH_3-4-C_6H_5]$_2TiCl_2$

Ti–Cl(1)	234.3(2)	Cl(1)–Ti–Cl(1A)	94.3(1)
Ti–C(1)	239.8(6)	CR(1)–Ti–CR(1A) [a]	127.5
Ti–C(2)	234.5(6)	PL(1)–PL(1A) [a]	56.3
Ti–C(3)	245.4(5)		
Ti–C(4)	242.1(5)	C(13)–C(1)–PL(1) [a]	5.3 (*exo*)
Ti–C(5)	241.3(6)	C(7)–C(3)–PL(1) [a]	5.3 (*exo*)
Ti–CR(1) [a]	208.0	C(6)–C(5)–PL(1) [a]	2.2 (*exo*)
C(13)–C(13A)	162.2(12)	C(14)–C(13)–C(13A)–C(15A)	23.8 (δ)
Cl(1A)···C(7)	310.2		
PLP–PL(1) [a]	13.4	TiCl(1)Cl(1A)–TiCR(1)CR(1A)	87.1
C(13)–C(1)–C(2) [a] (α_1)	122.4(6)	C(13)–C(1)–C(5) [a] (α_2)	131.2(7)
C(4)–C(5)–C(6) [a] (β_2)	121.1(6)	C(1)–C(5)–C(6) [a] (β_1)	131.3(6)

[a] CR = centroid, PL = mean plane of η^5-C_5 ring, PLP = mean plane of phenyl ring; for the definition of α_1, α_2, β_1 and β_2 see Scheme 4.

Accordingly, the out-of-plane bending of these aryl substituents (by $5 \pm 3°$, away from the metal centre) is significantly smaller than that ($10 \pm 2°$) found for bulky β-alkyl substituents. All of the aryl substituents are twisted relative to the adjacent C_5-ring plane, probably due to crystal packing effects, by angles of -30 to $+30°$. Both naphthyl residues of, e.g. **5b** are rotated "inward" (i.e. toward the Cl ligands) by ca $-30°$. A question to be settled by further studies concerns the degree to which there are mesomeric interactions between cyclopentadienyl and aryl rings in these complexes.

Table 3

Bonding and non-bonding distances (pm), bond and dihedral angles (°) with esd's in parentheses for complex **7a**, *rac*-$C_2(CH_3)_4$[1-R-(δ)-C_5H_2-2-CH_3-4-C_6H_5]$_2ZrCl_2$

Zr–Cl(1)	244.7(3)	Zr–CR(1) [a]	221.8
Zr–Cl(2)	244.2(3)	Zr–CR(2) [a]	221.6
Zr–C(1)	251.5(10)		
Zr–C(2)	249.9(9)	Cl(1)–Zr–Cl(2)	97.2(1)
Zr–C(3)	256.3(8)	CR(1)–Zr–CR(2) [a]	123.8
Zr–C(4)	254.1(8)	PL(1)–PL(2) [a]	59.0
Zr–C(5)	251.3(8)		
Zr–C(16)	251.0(9)	C(13)–C(1)–PL(1) [a]	4.8 (*exo*)
Zr–C(17)	249.9(9)	C(28)–C(16)–PL(2) [a]	5.3 (*exo*)
Zr–C(18)	257.1(9)	C(7)–C(3)–PL(1) [a]	4.5 (*exo*)
Zr–C(19)	252.8(8)	C(22)–C(18)–PL(2) [a]	2.8 (*exo*)
Zr–C(20)	251.1(8)	C(6)–C(5)–PL(1) [a]	2.2 (*exo*)
ZrCl(1)Cl(2)–ZrCR(1)CR(2) [a]	87.2	C(21)–C(20)–PL(2) [a]	2.4 (*exo*)
Cl(1)···C(22)	324.7	Cl(2)···C(7)	325.9
PLP(1)–PL(1) [a]	17.1	PLP(2)–PL(2) [a]	11.0
C(13)–C(28)	162.4(12)	C(1)–C(13)–C(28)–C(16)	32.0(10) (δ)
C(13)–C(1)–C(2) [a] (α_1)	122.5(8)	C(13)–C(1)–C(5) [a] (α_2)	130.7(9)
C(4)–C(5)–C(6) [a] (β_2)	120.2(8)	C(1)–C(5)–C(6) [a] (β_1)	131.8(9)
C(28)–C(16)–C(17) [a] (α_1)	121.8(8)	C(28)–C(16)–C(20) [a] (α_2)	131.3(8)
C(19)–C(20)–C(21) [a] (β_2)	119.2(8)	C(16)–C(20)–C(21) [a] (β_1)	132.4(9)

[a] CR = centroid, PL = mean plane of η^5-C_5 ring, PLP = mean plane of phenyl ring; for the definition of α_1, α_2, β_1 and β_2 see Scheme 4.

Table 4

Bonding and non-bonding distances (pm), bond and dihedral angles (°) with esd's in parentheses for complex **5b**, *rac*-$C_2(CH_3)_4$[1-C_5H_2-2-CH_3-4-(1-$C_{10}H_7$)]$_2TiCl_2$

Ti–Cl(1)	231.7(2)	Cl(1)–Ti–Cl(1A)	98.4(1)
Ti–C(1)	238.8(6)	CR(1)–Ti–CR(1A) [a]	130.3
Ti–C(2)	235.2(5)	PL(1)–PL(1A) [a]	54.7
Ti–C(3)	247.0(5)		
Ti–C(4)	243.5(5)	C(17)–C(1)–PL(1) [a]	5.6 (*exo*)
Ti–C(5)	240.1(6)	C(7)–C(3)–PL(1) [a]	6.7 (*exo*)
Ti–CR(1) [a]	208.8	C(6)–C(5)–PL(1) [a]	2.6 (*exo*)
C(17)–C(17A)	162.2(10)	C(18)–C(17)–C(17A)–C(19A)	19.2
Cl(1) ··· C(7)	311.6		
PLN–PL(1) [a]	34.3	TiCl(1)Cl(1A)–TiCR(1)CR(1A) [a]	87.1
C(17)–C(1)–C(2) [a] (α_1)	122.6(5)	C(17)–C(1)–C(5) [a] (α_2)	129.5(5)
C(4)–C(5)–C(6) [a] (β_2)	122.1(5)	C(1)–C(5)–C(6) [a] (β_1)	131.5(5)

[a] CR = centroid, PL = mean plane of η^5-C_5 ring, PLN = mean plane of naphthyl ring; for the definition of α_1, α_2, β_1 and β_2 see Scheme 4.

The conformations of the $(CH_3)_4C_2$ bridges in the phenyl-substituted complexes **5a** and **7a** (P for the 1*R*-configurated enantiomers) differ from those in related complexes with bulkier substituents [3,9,10] in that the phenyl groups lie in a "backward" position. For the naphthyl-substituted complex **5b** there is an eclipsed arrangement of the two C_5-ring ligands. A concomitant eclipsed conformation of the

Table 5

Bonding and non-bonding distances (pm), bond and dihedral angles (°) with esd's in parentheses for complex **8**, *rac*-$Si(CH_3)_2$[1-C_5H_2-2-CH_3-4-C_6H_5]$_2ZrCl_2$

Zr–Cl(1)	242.6(1)	Zr–CR(1) [a]	221.7
Zr–Cl(2)	242.9(1)	Zr–CR(2) [a]	223.2
Zr–C(1)	248.3(3)	Cl(1)–Zr–Cl(2)	98.6(1)
Zr–C(2)	248.6(4)	CR(1)–Zr–CR(2) [a]	126.0
Zr–C(3)	258.8(3)	C(1)–Si–C(13)	93.3(1)
Zr–C(4)	256.2(3)	C(25)–Si–C(26)	111.0(2)
Zr–C(5)	250.8(3)	PL(1)–PL(2) [a]	61.7
Zr–C(13)	247.9(3)		
Zr–C(14)	249.0(3)	Si–C(1)–PL(1) [a]	16.6 (*endo*)
Zr–C(15)	263.8(3)	Si–C(13)–PL(2) [a]	15.0 (*endo*)
Zr–C(16)	258.4(3)	C(7)–C(3)–PL(1) [a]	1.6 (*exo*)
Zr–C(17)	249.7(3)	C(19)–C(15)–PL(2) [a]	7.5 (*exo*)
Si–C(1)	188.0(3)	C(6)–C(5)–PL(1) [a]	2.1 (*exo*)
Si–C(13)	188.1(3)	C(18)–C(17)–PL(2) [a]	0.6 (*exo*)
Si–C(25)	186.1(4)		
Si–C(26)	183.5(4)	ZrCl(1)Cl(2)–ZrCR(1)CR(2) [a]	88.2
Cl(1) ··· C(19)	348.2	Cl(2) ··· C(7)	322.9
PLP(1)–PL(1) [a]	19.8	PLP(2)–PL(2) [a]	31.0
Si–C(1)–C(2) [a] (α_1)	120.7(3)	Si–C(1)–C(5) [a] (α_2)	128.7(3)
C(4)–C(5)–C(6) [a] (β_2)	124.1(3)	C(1)–C(5)–C(6) [a] (β_1)	128.6(3)
Si–C(13)–C(14) [a] (α_1)	118.6(2)	Si–C(13)–C(17) [a] (α_2)	131.4(3)
C(16)–C(17)–C(18) [a] (β_2)	124.3(3)	C(13)–C(17)–C(18) [a] (β_1)	128.2(3)

[a] CR = centroid, PL = mean plane of η^5-C_5 ring, PLP = mean plane of phenyl ring; for the definition of α_1, α_2, β_1 and β_2 see Scheme 4.

complex	α_1[a] [°]	α_2[a] [°]	β_1[a] [°]	β_2[a] [°]
5a	122	131	131	121
7a	122[b]	131[b]	132[b]	120[b]
5b	123	130	132	122
8	120[b]	130[b]	128[b]	124[b]

[a] rounded values; [b] averaged values for both η^5-C_5 rings

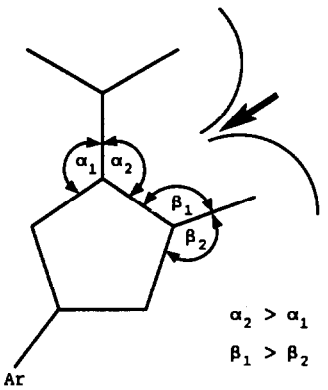

Scheme 4.

tetramethylethano bridge is avoided, however, by an in-plane bending of the bridgehead-bridge atom bond, away from the vicinal methyl group. Similar in-plane distortions due to non-bonding contacts between methyl groups at the bridge and at the α-ring position were also observed for the other complexes studied (Scheme 4).

Interestingly, three of the four chiral *ansa*-metallocene complexes studied, namely all three of the tetramethylethano-bridged species, crystallise in non-centrosymmetric space groups, i.e. as separate enantiomers. For two of these, complexes **5a** and **7a**, the absolute configuration of the enantiomers in the selected crystals could be determined by anomalous dispersion analysis; by chance the 1R configuration was observed in both cases. The spontaneous resolution of these complexes contrasts with the behaviour of other chiral *ansa*-metallocenes [3], for which the separated enantiomers are substantially more soluble than the corresponding racemate.

Discussion

The syntheses reported here show that aryl-substituted *ansa*-metallocene derivatives can be made by routes similar to those used for their alkyl-substituted congeners; the diastereoselectivity of the complex formation appears to be quite dependent, however, on the nature of counter-cation used to generate the ligand dianion. This observation, as well as the unselective formation of the dimethylsilano-bridged complexes **8** and **9**, has yet to be explained in terms of the stereo-controlling transition state of these complex formation reactions.

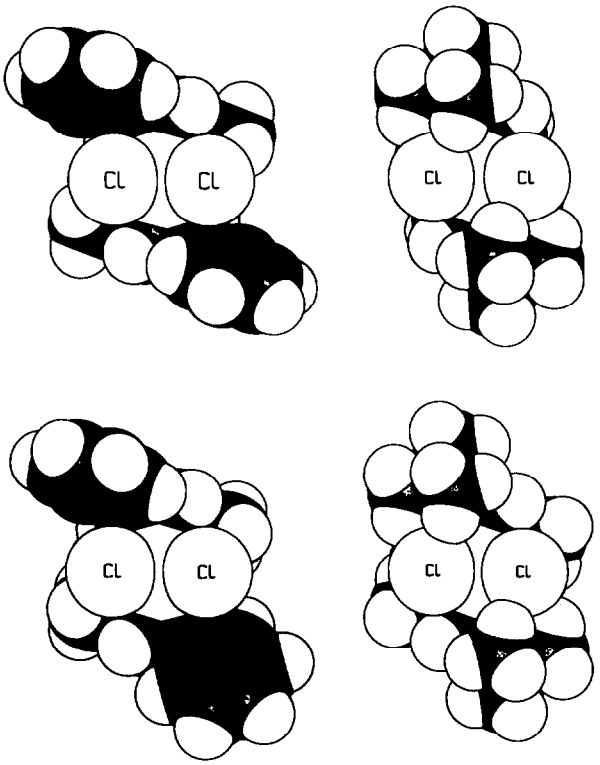

Fig. 5. Space-filling models for chiral *ansa*-zirconocenes with β-aryl and with β-alkyl substituents. Top row: Complex **7a** (left) and its β-t-butyl, 2-normethyl analogue [9] (right); bottom row: Complex **8** (left) and its β-t-butyl analogue [7] (right).

The most striking feature of the aryl-substituted, chiral *ansa*-metallocene derivatives reported here is the presence of a much more openly accessible coordination site [15] than in comparable complexes with tertiary alkyl substituents (Fig. 5). In accord with this, very high activities as α-olefin polymerisation catalysts are observed for these aryl-substituted complexes [16]: After activation with poly(methylalumoxane) [17], complex **8**, e.g., catalyses (at 50 °C and 2 bar propene pressure) the polymerisation of propene at a rate of ca. 125 insertions per second. This rate is about 50 times higher than that observed for its t-butyl congener shown in Fig. 5.

Experimental

Unless otherwise stated, all reactions were carried out under argon by standard Schlenk techniques, with solvents thoroughly dried and degassed. 1-Naphthyllithium · TMEDA was prepared as previously described [18]. 3-Methyl-2-cyclopentene-1-one (Fluka No. 66545) and dichlorodimethylsilane (Aldrich No. D6,082-6) were distilled prior to use. A 1.6 *M* solution of n-butyllithium in hexane (Metallgesellschaft) was used as purchased.

Table 6

^{1}H NMR data for the 3-*R*-1-methylcyclopentadienes (**1a,b**, mixture of the tautomers) in $CDCl_3$ at 25 °C, δ in ppm (relative to $\delta(CHCl_3)$ 7.24 ppm) at 250 MHz (ump = unresolved multiplet, m = multiplet)

R = phenyl (**1a**)	R = 1-napthyl (**1b**)		
1.95–2.06	2.08–2.11	(m,3)	3-CH_3
3.00,3.21,3.28		(ump,2)	C_5H_4 (CH_2)
	3.12–3.14,3.44–3.46	(m,2)	C_5H_4 (CH_2)
5.93,6.10,6.67		(ump,2)	C_5H_4 (CH)
	6.06–6.11,6.28–6.32	(m,2)	C_5H_4 (CH)
	6.39–6.43,6.61–6.67		
7.05–7.24		(m,5)	1-C_6H_5
	7.32–7.34	(m,4)	1-(1-$C_{10}H_7$)
	7.66–7.84	(m,2)	1-(1-$C_{10}H_7$)
	8.10–8.16,8.24–8.28	(m,1)	1-(1-$C_{10}H_7$)

Synthesis of 1-aryl-3-methylsubstituted cyclopentadienes (1a,b)

3-Methyl-1-phenylcyclopentadiene (**1a**) was prepared by a modification of a procedure described in the literature [11], avoiding acidic conditions during work-up. Reaction of phenyllithium with 3-methyl-2-cyclopentene-1-one and thermal dehydration of the alcohol essentially as described for the synthesis of phenylcyclopentadiene [12] gave the desired cyclopentadiene as a white solid in about 80% yield (mp. 60 °C; lit. 59–62 °C [19,20]). 1-(1-Napthyl)-3-methyl-cyclopentadiene (**1b**) was prepared similarly by the reaction of equimolar amounts of 1-lithio-naphthalin · TMEDA with 3-methyl-2-cyclopentene-1-one in diethyl ether. Dehydration of the alcohol was carried out either by use of catalytic amounts of *p*-toluenesulfonic acid in diethyl ether or thermally at 180 °C *in vacuo*, to yield the 1,3-disubstituted cyclopentadiene **1b** as a yellow oil in ca. 65% yield. For ^{1}H NMR data see Table 6.

Ligand syntheses (3a,b,4)

(A) C_2-bridged ligands (3a,b). The 1,3-disubstituted fulvenes **2a,b** required for reductive coupling were prepared in ca. 90% yield by the pyrrolidine-induced condensation (cf. ref. 13) of the appropriate cyclopentadienes **1a,b** with the stoichiometric amount of acetone in methanol/ether (10/1). After neutralisation with acetic acid and addition of water, the fulvenes were extracted into diethyl ether/pentane (1/1), and the extract was washed several times with water, dried over anhydrous $MgSO_4$ and evaporated to dryness. The fulvenes **2a,b** (yellow to orange oils) showed no signals from impurities in their 250 MHz ^{1}H NMR spectra, and were used without further purification for the reductive dimerisation with Mg/CCl_4. The ^{1}H NMR data are presented in Table 7.

With the following modifications of the literature procedure [8,9], the novel fulvenes **2a,b** were reductively coupled with Mg/CCl_4 in THF to give the desired di-Grignard derivatives **3a,b**. As the products are soluble in THF, half of the solvent had to be removed *in vacuo*; upon addition of diethyl ether the ligand salts separated *. These were collected by filtration, washed with pentane and diethyl

* Addition of pentane to the reaction mixture leads to the formation of brown insoluble resins and so should be avoided.

Table 7

^{1}H-NMR data for the 3-R-1,6,6-trimethylfulvenes (**2a,b**) in $CDCl_3$ at 25 °C, δ in ppm (relative to δ ($CHCl_3$) 7.24 ppm) at 250 MHz (s = singlet, d = doublet, ump = unresolved multiplet, m = multiplet, J(1-CH_3,H2) 1.5, J(H4,H2) 2.0 Hz)

R = phenyl (**2a**)	R = 1-napthyl (**2b**)		
2.34	2.31	(s,3)	6,6-C(CH_3)$_2$
2.39	2.38	(d,3)	1-CH_3
6.68	6.55	(ump,1)	2-C_5H_2
6.80	6.65	(d,1)	4-C_5H_2
7.27–7.69		(m,5)	3-C_6H_5
	7.30–7.47	(m,6)	3-(1-$C_{10}H_7$)
	8.27–8.31	(m,1)	3-(1-$C_{10}H_7$)

ether, then dried *in vacuo* to give the desired products **3a,b** as white air-sensitive solids in ca. 15% yield.

(B) $SiMe_2$-bridged ligand (4). A solution of 7.8 g (50 mmol) of 3-methyl-1-phenylcyclopentadiene (**1a**) in 125 ml of THF, was treated with n-butyllithium (50 mmol) at 0 °C. The mixture was allowed to warm to room temperature and a solution of dichlorodimethylsilane (23 mmol) in 40 ml THF was slowly added. The mixture was stirred for 2 d, then cooled to 0 °C and 28 ml (44 mmol) of a 1.6 *M* solution of n-butyllithium was slowly added. The mixture was then allowed to warm to room temperature during overnight stirring. The solution of the dilithium salt of the ligand **4** was used without further purification for the synthesis of the *ansa*-zirconocene complexes (**8** and **9**).

Syntheses of the ansa-metallocenes (5a,b,6,7a,8,9)

1. $C_2(CH_3)_4[1\text{-}C_5H_2\text{-}2\text{-}CH_3\text{-}4\text{-}C_6H_5]_2TiCl_2$ (5a (rac), 6 (meso))

(A) By reaction of $C_2(CH_3)_4[1\text{-}C_5H_2\text{-}2\text{-}CH_3\text{-}4\text{-}C_6H_5MgCl]_2 \cdot 4THF$ (3a) with $TiCl_3 \cdot 3THF$. A solution of 7.2 g of (9 mmol) $C_2(CH_3)_4[1\text{-}C_5H_2\text{-}2\text{-}CH_3\text{-}4\text{-}C_6H_5MgCl]_2 \cdot 4THF$ (**3a**) in 150 ml of THF was cooled to −78 °C, 3.4 g (9 mmol) of $TiCl_3 \cdot 3THF$ were added, and the mixture was allowed to warm to room temperature, then kept for 16 h under reflux. It was then cooled to −40 °C and 2.5 ml (12.5 mmol) of 5 *M* aqueous HCl were added and the mixture was stirred under air for 4 h during which the solution turned red. The solution was evaporated to dryness and the viscous residue was taken up in a small amount of CH_2Cl_2/diethyl ether (1/2) and the solution filtered through a short column ($\varnothing$ = 2 cm, h = 10 cm) of acidic alumina (Merck A90, activity I, No. 1078.1000). The unchanged ligand was eluted first (yellow band); then a red band containing the two diastereomers (*rac* (**5a**) and *meso* (**6**)) was collected and the solvent removed *in vacuo* to give a red, slightly oily solid. The ^{1}H NMR spectrum of the crude product showed a ratio of 6/1 for the diastereomers in favour of the racemic species. The product was freed from oily impurities by adsorptive filtration over flash silica gel (J.T. Baker, No. 7024-1) with diethyl ether as eluent. After removal of the solvent and recrystallisation from diethyl ether, 0.7 g (1.35 mmol, 15%) of the diastereomers were obtained in analytically pure form. Repeated fractional crystallisation from diethyl ether at −80 °C yielded pure racemic diastereomer **5a**. The product was identified from its

mass spectrum (parent ion at *m/e* 510–515 with appropriate isotope pattern) and an elemental analysis: Found: C, 69.91; H, 6.29; $C_{30}H_{32}TiCl_2$ (511.4) calc: C, 70.46; H, 6.31%. The ^1H NMR data are listed in Table 1; the results of an X-ray crystal structure determination of the racemic compound **5a** are described below.

(B) From $C_2(CH_3)_4[1\text{-}C_5H_2\text{-}2\text{-}CH_3\text{-}4\text{-}C_6H_5Li]_2$ with $TiCl_3 \cdot 3THF$. A solution of 6.3 g (17 mmol) of ($C_2(CH_3)_4[1\text{-}C_5H_3\text{-}2\text{-}CH_3\text{-}4\text{-}C_6H_5]_2$) (**3a**) in 80 ml THF was cooled to −30 °C and of 23 ml (37 mmol) of a 1.6 *M* solution of n-butyllithium was added. The mixture was stirred for 3 h at −30 °C, then for a further 2 h at room temperature. It was then cooled to −78 °C and 6.3 g (17 mmol) of $TiCl_3 \cdot 3THF$ were added. The mixture was allowed to warm to room temperature, then heated for 20 h under reflux. Further work-up was carried out as described under (A). Yield: 2.5 g (**5a** + **6**, 4.9 mmol), 29% theoretical yield; mixture of the meso and racemic diastereomer; ratio 2/1 (*rac/meso*).

(C) From $C_2(CH_3)_4[1\text{-}C_5H_2\text{-}2\text{-}CH_3\text{-}4\text{-}C_6H_5MgCl]_2 \cdot 4THF$ (3a) with $TiCl_4$ in toluene. A suspension of 5.3 g (6.6 mmol) of the di-Grignard compound **3a** in 150 ml toluene was cooled to 0 °C. Upon addition of 6.6 ml (6.6 mmol) of a 1 *M* solution of $TiCl_4$ in toluene the supernatant solution immediately turned red. The mixture was allowed to warm to room temperature, then kept for 12 h under reflux. The organic phase was washed three times with 50 ml of diluted HCl, dried over anhydrous $MgSO_4$, and evaporated to dryness. Further work-up was carried out as described for the analogous reaction of $TiCl_3 \cdot 3THF$ (see under (A)). 1.4 g (2.7 mmol), 40% of the diastereomers **5a**, **6** were obtained with a *rac/meso* ratio of 1.

(2) Synthesis of $(C_2(CH_3)_4[1\text{-}C_5H_2\text{-}2\text{-}CH_3\text{-}4\text{-}C_6H_5]_2ZrCl_2)$ (7a)

A solution of 6.6 g (8.2 mmol) of $C_2(CH_3)_4[1\text{-}C_5H_2\text{-}2\text{-}CH_3\text{-}4\text{-}C_6H_5MgCl]_2 \cdot 4THF$ (**3a**) in 100 ml of THF was cooled to −78 °C. After addition of 3.1 g (8.2 mmol) $ZrCl_4 \cdot 2THF$ the mixture was allowed to warm to room temperature and then heated for 24 h under reflux. After removal of the solvent the yellow-brown oily residue was taken up in CH_2Cl_2/diethyl ether (1/1) and the solution filtered through a pad of Celite. The desired zirconocene complex was obtained in pure racemic form by several recrystallisations from this solvent mixture. Yield: 0.46 g (0.84 mmol), 10%. The identity of **7a** was confirmed by its mass spectrum (parent ion at *m/e* 552–557 with appropriate isotope distribution) and an X-ray crystal structure determination (see next section). For ^1H NMR data see Table 1.

(3) Synthesis of $(C_2(CH_3)_4[1\text{-}C_5H_2\text{-}2\text{-}CH_3\text{-}4\text{-}(1\text{-}C_{10}H_7)]_2TiCl_2)$ (5b)

With the modifications described below, a procedure similar to that described for the synthesis of **5a**, **6** (see under 1(A)) gave the naphthyl-substituted complex **5b**. Adsorptive filtrations were carried out with diethyl ether (without CH_2Cl_2) as eluent. The product was recrystallised from diethyl ether at −30 °C to give the red *ansa*-titanocene complex **5b** analytically pure and without admixture with the *meso* isomer in 8% yield. **5b** was identified from its mass spectrum (parent ion 610–615 with the expected isotope pattern) and elemental analysis: Found: C, 74.07, H, 6.05. $C_{38}H_{36}TiCl_2$ (611.5) calc: C, 74.64; H, 5.93%. The ^1H NMR spectrum (Table 1) is consistent with results of an X-ray crystal structure determination for **5b** (see next section).

*(4) Synthesis of $Si(CH_3)_2[1\text{-}C_5H_2\text{-}2\text{-}CH_3\text{-}4\text{-}C_6H_5]_2ZrCl_2$ (**8** (rac), **9** (meso))*

The THF solution of the dilithium salt of the ligand **4**, prepared *in situ* from 7.8 g (50 mmol) 3-methyl-1-phenylcyclopentadiene (**1a**) and 23 mmol $SiMe_2Cl_2$ (see ligand synthesis (B)), was cooled to −78 °C and 7.2 g (19 mmol) $ZrCl_4 \cdot 2THF$ were added. The stirred suspension was allowed to warm slowly to room temperature, stirred for a further 2 d, then evaporated to dryness. The yellow residue was taken up in 60 ml of toluene and the solution filtered to remove LiCl. After partial evaporation of the solvent the product was isolated by crystallisation at −80 °C to yield 0.63 g of the diastereomers (*rac/meso* 1/2). A further crop (0.57 g, rac/meso 2/1) was obtained by slow diffusion of pentane into the mother liquor. Total yield: 1.2 g (2.3 mmol) 12% with a *rac/meso* mixture close to 1. The diastereomers **8,9** were identified by their ^1H NMR spectra (Table 1) and by an X-ray crystal structure determination of racemic zirconocene complex **8** (see next section).

Crystal structure determinations

Space groups, cell parameters and X-ray diffraction intensities for suitable crystals of the racemic *ansa*-metallocenes were determined on a Syntex-P3 four circle diffractometer (Mo-K_α, λ 71.069 pm, graphite monochromator, ω-scan with $\Delta\omega$ 1.5° for **5a**, **7a**, 0.7° for **5b** and 1.6° for **8**; $2.0 \leq \omega \leq 29.3°$ min^{-1} for *rac*-**5a**, **5b**, **7a**, and $2.3 \leq \omega \leq 29.3°$ min^{-1} for **8**; $4.0 \leq 2\theta \leq 52°$ for **5a**, **7a**, $4.0 \leq 2\theta \leq 55°$ for **5b** and $4.0 \leq 2\theta \leq 54°$ for **8**).

Single crystals of **5a** (*rac-R-*(δ)) suitable for X-ray diffraction were obtained by slow crystallisation from CH_2Cl_2/pentane. Data collected at 206 K showed the crystals to be monoclinic, space group *C*2 (No. 5) with *a* 1594.8(3), *b* 932.1(2), *c* 1021.7(2) pm, β 113.88(3)°; *V* 1389×10^6 pm^3; two molecules of CH_2Cl_2 were

Table 8

Fractional coordinates ($\times 10^4$) (with esd's) and isotropic parameters ($pm^2 \times 10^{-1}$) for complex **5a** (*rac*-$C_2(CH_3)_4[1\text{-}C_5H_2\text{-}2\text{-}CH_3\text{-}4\text{-}C_6H_5]_2TiCl_2$) with one molecule of CH_2Cl_2 per asymmetric unit

Atom	*x*	*y*	*z*	U^a
Ti(1)	5000	5000	5000	20(1)
Cl(1)	4520(1)	6710(2)	6232(2)	30(1)
C(1)	4104(4)	2860(7)	4177(7)	24(2)
C(2)	4256(4)	3501(7)	3023(6)	24(2)
C(3)	3757(4)	4822(7)	2603(6)	22(2)
C(4)	3361(3)	5038(8)	3589(6)	24(2)
C(5)	3554(4)	3849(7)	4551(7)	24(2)
C(6)	3158(5)	3766(8)	5649(8)	37(3)
C(7)	3639(4)	5721(7)	1370(7)	25(2)
C(8)	3900(5)	5219(8)	318(8)	37(3)
C(9)	3761(6)	6042(9)	−872(10)	48(3)
C(10)	3346(5)	7367(9)	−1052(8)	44(3)
C(11)	3088(5)	7883(9)	0(9)	45(3)
C(12)	3235(4)	7063(8)	1200(8)	35(3)
C(13)	4447(4)	1354(7)	4731(7)	24(2)
C(14)	4001(4)	308(7)	3481(8)	34(3)
C(15)	4132(5)	870(7)	5867(8)	33(3)
C(16)	5000	112(14)	0	45(4)
Cl(2)	4006(2)	1191(3)	−509(3)	60(1)

[a] Equivalent isotropic *U* defined as one third of the orthogonalised U_{ij} tensor.

present per unit cell, to give with $Z = 2$ a crystallographic density $d_{calc.}$ of 1.43 g/cm^3. For resolution and refinement of the structure 1341 independent reflections with $I \geq 3\sigma(I)$ were used without absorption corrections. The structure was solved by the Patterson method (SHELXTL PLUS). For refinement the titanium atom was fixed on a crystallographic C_2-axis at position 1/2, 1/2, 1/2. Refinement, using a unit weighting scheme, was anisotropic except for H atoms which were held in calculated positions; it converged at R_1 * 0.041 and R_2 * 0.053 with a goodness-of-

* $R_1 = (\Sigma | |F_o| - |F_c| |)/\Sigma |F_o|$ and $R_2 = [\Sigma\omega(|F_o| - |F_c|)^2]^{1/2}/[\Sigma\omega |F_o|^2]^{1/2}$.

Table 9

Fractional coordinates ($\times 10^4$) (with esd's) and isotropic parameters (pm$^2 \times 10^{-1}$) for **7a** (*rac*-$C_2(CH_3)_4[1\text{-}C_5H_2\text{-}2\text{-}CH_3\text{-}4\text{-}C_6H_5]_2ZrCl_2$) with one molecule of CH_2Cl_2 per asymmetric unit

Atom	x	y	z	U^a
Zr(1)	1957(1)	989(1)	1252(1)	17(1)
Cl(1)	3652(3)	2598(2)	981(1)	26(1)
Cl(2)	3681(3)	−608(2)	1508(1)	26(1)
C(1)	−277(11)	664(9)	801(3)	24(3)
C(2)	339(10)	−573(9)	866(3)	20(3)
C(3)	1630(11)	−668(9)	612(3)	20(3)
C(4)	1806(12)	544(9)	401(3)	24(3)
C(5)	664(11)	1367(9)	515(3)	19(3)
C(6)	573(11)	2720(10)	311(3)	27(3)
C(7)	2502(12)	−1813(10)	555(3)	25(3)
C(8)	2032(14)	−3034(9)	670(3)	31(3)
C(9)	2819(16)	−4131(11)	590(3)	43(4)
C(10)	4168(13)	−4040(12)	422(4)	39(4)
C(11)	4696(12)	−2814(12)	303(3)	39(4)
C(12)	3905(12)	−1737(10)	374(3)	30(3)
C(13)	−1743(10)	1021(9)	990(3)	22(3)
C(14)	−2817(13)	72(11)	782(3)	31(3)
C(15)	−2239(11)	2382(10)	838(3)	28(3)
C(16)	−240(11)	1279(9)	1721(3)	21(3)
C(17)	351(10)	2529(9)	1654(3)	21(3)
C(18)	1643(11)	2641(9)	1897(3)	22(3)
C(19)	1883(12)	1414(9)	2100(3)	23(3)
C(20)	725(11)	590(9)	1997(3)	20(3)
C(21)	686(12)	−773(9)	2203(3)	30(3)
C(22)	2543(11)	3778(9)	1943(3)	25(3)
C(23)	2142(13)	4985(10)	1798(3)	35(4)
C(24)	2947(16)	6083(11)	1849(3)	43(4)
C(25)	4303(15)	5978(12)	2039(4)	43(4)
C(26)	4761(14)	4784(12)	2189(3)	43(4)
C(27)	3907(12)	3700(10)	2136(3)	31(3)
C(28)	−1741(11)	923(10)	1543(3)	25(3)
C(29)	−2830(13)	1859(10)	1763(3)	34(4)
C(30)	−2184(13)	−434(11)	1702(3)	35(4)
C(31)	3051(13)	923(13)	3779(3)	49(4)
Cl(3)	1974(4)	1033(3)	4284(1)	49(1)
Cl(4)	1899(4)	902(3)	3292(1)	51(1)

[a] Equivalent isotropic U defined as one third of the orthogonalised U_{ij} tensor.

fit of 1.78. Refinement with the mirror-image configuration e.g. *rac*-*S*-(λ)-**1**-$TiCl_2$ gave significantly higher R_1 and R_2 values. Structural parameters for *rac*-*R*-(δ)-**1**-$TiCl_2$ are presented in Table 8.

Single crystals of **7a** (*rac*-*R*-(δ)) suitable for an X-ray crystallographic determination were obtained by slow diffusion of diethyl ether into a dichloromethane solution. The crystals are orthorhombic, space group $P2_12_12_1$ (No. 19); *a* 945.3(2), *b* 1037.2(2), *c* 2933.3(7) pm; 4 molecules (+4 molecules of CH_2Cl_2) per unit cell, *V* 2876×10^6 pm^3; $d_{calc.}$ 1.48 g/cm^3. Of 2849 intensities measured, 2504 independent reflections with $I \geq 5\sigma(I)$ were used for resolution and refinement without absorption corrections. The structure was solved by direct methods (SHELXS86) and refined (SHELX76) with hydrogen atoms in calculated positions. Anisotropic refinement for other atoms using a weighting scheme of $\omega^{-1} = \sigma^2(F) + 0.0002F^2$ converged at R_1 0.0612 and R_2 0.0740 (goodness-of-fit 3.52). The absolute configuration of the complex was shown to be 1-*R*-(δ) by refinement of the mirror-image configuration, which gave significantly higher R_1 and R_2 values. Structural parameters for **7a** are presented in Table 9.

Single crystals of **5b** suitable for an X-ray crystallographic determination were obtained by slow evaporation of a diethyl ether solution. The crystals (data collected at 227 K) are tetragonal, space group $P4_32_12$ (No. 96) with *a* 878.0(4), *c* 4004.8(14) pm; *V* 3088×10^6 pm^3; 4 crystallographically equivalent molecules were found per unit cell, giving a crystallographic density $d_{calc.}$ of 1.39 g/cm^3. For resolution and refinement 3054 independent reflections with $I \geq 6\sigma(I)$ were used. The structure

Table 10

Fractional coordinates ($\times 10^4$) (with esd's) and isotropic parameters (pm$^2 \times 10^{-1}$) for complex **5b** (*rac*-$C_2(CH_3)_4$[1-C_5H_2-2-CH_3-4-(1-$C_{10}H_7$)]$_2TiCl_2$)

Atom	*x*	*y*	*z*	*U* [a]
Ti(1)	−187(1)	−187(1)	0	19(1)
Cl(1)	2435(2)	−370(2)	52(1)	31(1)
C(1)	−1886(7)	−1643(7)	339(1)	22(2)
C(2)	−396(7)	−1862(7)	456(1)	22(2)
C(3)	138(6)	−492(7)	609(1)	21(2)
C(4)	−1027(7)	582(7)	554(1)	23(2)
C(5)	−2270(7)	−79(7)	387(1)	22(2)
C(6)	−3689(7)	775(7)	320(1)	31(2)
C(7)	1540(7)	−347(8)	805(1)	26(2)
C(8)	2013(8)	−1615(8)	978(1)	37(2)
C(9)	3274(9)	−1589(9)	1198(2)	47(3)
C(10)	4051(8)	−267(10)	1233(2)	46(3)
C(11)	3655(8)	1040(9)	1066(1)	40(2)
C(12)	4497(9)	2395(10)	1104(2)	49(3)
C(13)	4166(9)	3667(9)	936(2)	57(3)
C(14)	2957(8)	3663(8)	708(2)	42(2)
C(15)	2115(8)	2394(8)	659(2)	38(2)
C(16)	2398(7)	1059(8)	840(1)	31(2)
C(17)	−2868(7)	−2955(7)	202(1)	26(2)
C(18)	−2202(8)	−4491(7)	322(1)	35(2)
C(19)	−4450(7)	−2865(8)	370(1)	35(2)

[a] Equivalent isotropic *U* defined as one third of the orthogonalised U_{ij} tensor.

Table 11

Fractional coordinates ($\times 10^4$) (with esd's) and isotropic parameters ($pm^2 \times 10^{-1}$) for complex **8** (*rac*-$Si(CH_3)_2[1\text{-}C_5H_2\text{-}2\text{-}CH_3\text{-}4\text{-}C_6H_5]_2ZrCl_2$)

Atom	x	y	z	U^a
Zr(1)	2702(1)	7084(1)	2595(1)	23(1)
Cl(1)	19(1)	7200(1)	2638(1)	38(1)
Cl(2)	2823(1)	9478(1)	2954(1)	32(1)
Si(1)	5467(1)	4454(1)	2187(1)	27(1)
C(1)	4212(4)	4933(3)	3317(2)	28(1)
C(2)	4465(4)	6090(3)	3809(2)	27(1)
C(3)	3142(4)	6520(3)	4425(2)	30(1)
C(4)	2072(4)	5682(3)	4284(2)	31(1)
C(5)	2689(4)	4699(3)	3608(2)	29(1)
C(6)	1862(5)	3594(3)	3330(3)	42(1)
C(7)	2960(5)	7644(3)	5089(2)	31(1)
C(8)	4165(5)	8095(3)	5390(2)	35(1)
C(9)	3995(5)	9160(4)	6008(3)	43(1)
C(10)	2577(6)	9770(4)	6317(3)	46(2)
C(11)	1356(5)	9331(4)	6027(3)	45(1)
C(12)	1509(5)	8276(3)	5398(2)	36(1)
C(13)	4633(4)	6023(3)	1379(2)	28(1)
C(14)	3232(4)	5951(3)	1048(2)	26(1)
C(15)	2586(4)	7328(3)	683(2)	26(1)
C(16)	3564(4)	8270(3)	854(2)	28(1)
C(17)	4814(4)	7502(3)	1280(2)	26(1)
C(18)	6077(4)	8168(4)	1528(3)	36(1)
C(19)	1292(4)	7642(3)	138(2)	28(1)
C(20)	1201(5)	8796(3)	−603(2)	34(1)
C(21)	35(5)	9029(4)	−1174(3)	40(1)
C(22)	−1066(5)	8145(4)	−1016(3)	39(1)
C(23)	−1001(5)	7014(4)	−282(3)	37(1)
C(24)	162(5)	6763(3)	286(3)	33(1)
C(25)	5126(5)	2811(3)	1715(3)	37(1)
C(26)	7447(4)	4425(4)	2320(3)	38(1)

[a] Equivalent isotropic U defined as one third of the orthognalised U_{ij} tensor.

was solved by direct methods (SHELXS86); the titanium atom is located on a crystallographic C_2-axis. Refinement (SHELX76) with H atoms in calculated positions but other atoms anisotropically, using a weighting scheme of $\omega^{-1} = \sigma^2(F) + 0.0000F^2$ converged at R_1 0.0897 and R_2 0.0691 (goodness-of-fit 3.91). Structural parameters for **5b** are presented in Table 10.

Single crystals (yellow) of **8** suitable for an X-ray crystallographic determination were obtained by slow diffusion of pentane into a toluene solution. The crystals (data collected at 223 K) are triclinic, space group $P\bar{1}$ (No. 2) with a 911.5(4), b 956.6(3), c 1383.0(5) pm, α 82.10(3), β 82.22(3), γ 82.23(3)°; V 1175×10^6 pm^3; 2 crystallographically equivalent molecules were found per unit cell; $d_{calc.}$ 1.49 g/cm^3. Of 3777 reflections collected, 3352 with $I \geq 3\sigma(I)$ were used for resolution and refinement without absorption corrections. The structure was solved by the Patterson method (SHELXTL PLUS). For refinement (SHELXTL PLUS) hydrogen atoms were kept in calculated positions but other atoms treated anisotropically (unit weighting

scheme). Refinement converged at R_1 0.0289 and R_2 0.0323. The structural parameters are presented in Table 11 *.

Acknowledgements

We thank Dr. M. Wiebcke for helpful comments on X-ray crystal structure determinations. Financial support for this study by Stiftung Volkswagenwerk, by Fonds der Chemischen Industrie and by funds of the University of Konstanz is gratefully acknowledged.

References

1 P. Pino, P. Cioni and J. Wei, J. Am. Chem. Soc., 109 (1987) 6189; P. Pino, P. Cioni, M. Galimberti, J. Wei and N. Piccolrovazzi, in W. Kaminsky and H. Sinn (Eds.), Transition Metals and Organometallics as Catalysts for Olefin Polymerisation, Springer-Verlag, Berlin, 1988, p. 269; P. Pino and M. Galimberti, J. Organomet. Chem., 370 (1989) 1; R. Waymouth and P. Pino, J. Am. Chem. Soc., 112 (1990) 4911.
2 W. Kaminsky, K. Külper, H.H. Brintzinger and F.R.W.P. Wild, Angew. Chem., 97 (1985) 507.
3 A. Schäfer, E. Karl, L. Zsolnai, G. Huttner and H.H. Brintzinger, J. Organomet. Chem., 328 (1987) 87.
4 P. Corradini, G. Guerra, M. Vacatello and V. Villani, Gazz. Chim. Ital., 118 (1988) 173.
5 S. Miya, T. Yoshimura, T. Mise and H. Yamazaki, Polymer Prepr. Jpn., 37 (1988) 285; T. Mise, S. Miya and H. Yamazaki, Chem. Lett., (1989) 1853.
6 W. Röll, H.H. Brintzinger, B. Rieger and R. Zolk, Angew. Chem., 102 (1990) 339.
7 H. Wiesenfeldt, A. Reinmuth, E. Barsties, K. Evertz and H.H. Brintzinger, J. Organomet. Chem., 369 (1989) 359.
8 H. Schwemlein and H.H. Brintzinger, J. Organomet. Chem., 254 (1983) 69.
9 S. Gutmann, P. Burger, H.U. Hund, J. Hofmann and H.H. Brintzinger, J. Organomet. Chem., 369 (1989) 343.
10 S. Collins, Y. Hong and N.J. Taylor, Organometallics, 9 (1990) 2695.
11 F.H. Köhler and G.E. Matsubayashi, Chem. Ber., 109 (1976) 329.
12 R. Riemschneider and R. Nerin, Monatsh. Chem., 91 (1960) 829.
13 K.J. Stone and R.D. Little, J. Org. Chem., 49 (1984) 1849.
14 S. Gutmann, P. Burger, M.H. Prosenc and H.H. Brintzinger, J. Organomet. Chem., 397 (1990) 21.
15 H. Hortmann and H.H. Brintzinger, New J. Chem., in press.
16 A. Reinmuth, W. Röll, B. Rieger and H.H. Brintzinger, in preparation.
17 W. Kaminsky, M. Miri, H. Sinn and R. Woldt, Makromol. Chem. Rapid Commun., 4 (1983) 417.
18 W. Neugebauer, T. Clark and P. v. R. Schleyer, Chem. Ber., 116 (1983) 3283.
19 W. Borsche and W. Menz, Ber., 41 (1908) 190.
20 R.F. Heck, J. Org. Chem., 30 (1965) 2205.

* Structural data obtained for these four compounds are available on request from Fachinformationszentrum Karlsruhe, Gesellschaft für wissenschaftlich-technische Information mbH, W-7514 Eggenstein-Leopoldshafen 2, upon quotation of deposit number CSD-55375, the authors, and the journal reference for this article.